phys. stat. sol. (c) **1**, No. S2, S202–S209 (2004) / **DOI** 10.1002/pssc.200405141

Photonic devices based on wide gap semiconductors for room temperature polariton emission

A. Pawlis[*], **D. J. As, D. Schikora, J. Schörmann,** and **K. Lischka**

Faculty of Science, Department of Physics, University of Paderborn, Warburger Str. 100, 33098 Paderborn, Germany

Received 25 March 2004, revised 15 June 2004, accepted 17 June 2004
Published online 1 September 2004

PACS 71.35.Gg, 71.35.–y, 71.36.+c, 71.55.Gs, 78.30.Fs

Planar semiconductor microcavities have found increasing attention since they allow to enhance and control the interaction between light and excitons. When the coupling between photon and exciton is strong enough, polaritons are formed which are observed in a pronounced Rabi-splitting in the cavity spectra. The strong exciton-light coupling regime, necessesary for polariton-based applications depends on the oscillator strength and the exciton binding energy. The wide-gap II–VI (CdTe,ZnSe and CdSe) as well as the group III-nitrides (GaN,InN and AlN) semiconductors excellently fulfil these conditions. We observed a large Rabi-splitting (about 44 meV) with ZnSe-based semiconductor microcavities containing four strained (Zn,Cd)Se quantum wells and ZnS/YF_3 distributed Bragg-reflectors. Measurements of the reflectivity and of the photoluminescence revealed clear evidence of the strong coupling regime. We also report on first experiments to optimise the structural and optical properties of (Al,Ga)N/GaN quantum wells. The results obtained so far show that these structures may be used for the investigation of polariton Rabi-splitting at room temperature.

1 Introduction

Semiconductor quantum wells as part of microcavities allow to study the interconversion between excitons and photons. In the strong-coupling regime this interaction is manifested by new quantum mechanical eigenstates, the so-called polaritons, which show some extraordinary optical properties. One of these properties is an "anti-crossing" behaviour of the polariton dispersion, which forms an upper and lower polariton band. The minimal energy difference between these bands is the Rabi-splitting energy $\hbar\Omega_{\mathrm{Rabi}}$, which is observed in resonance between the cavity mode and the exciton transition. The physical properties of microcavity polaritons open up the possibility to develop new types of efficient light emitters and quantum processors [1, 2].

For room temperature applications the Rabi-splitting energy must exceed the thermal energy of about 25 meV. Most promising candidates for such applications are ZnSe and CdSe (green/blue spectral range) as well as GaN, InN and AlN (blue/near UV spectral range), since $\hbar\Omega_{\mathrm{Rabi}}$ is proportional to the oscillator strength f_{osz} of the quantum structure [3].

After the first observation of a polariton splitting in a Fabry-Perot microcavity (Weisbuch et. al. 1992) [4, 5], the strong coupling regime was studied in several III-V and II-VI semiconductor microcavities [6–9]. Kelkar et al. [10] reported a Rabi-splitting of 17.5 meV at 70 K and 10 meV at 175 K in a (Zn,Mg)(S,Se) microcavity with three (Zn,Cd)Se quantum wells as the resonant medium and dielectric Bragg-mirrors of SiO_2/TiO_2. André et al. [11] investigated CdTe multi quantum well structures enclosed in (Cd,Mg)Te/(Cd,Mn)Te semiconductor Bragg-mirrors, showing room temperature Rabi-splitting ener-

[*] Corresponding author: e-mail: LI_XP@PHYSIK.UNI-PADERBORN.DE

gies between 12 meV and 30 meV as a function of the number of quantum wells. Recently Saba et al. [12, 13] have measured parametric polariton amplification up to 220 K in CdTe based multi quantum well microcavity structures. The experimental observations demonstrate that the polariton amplification cut-off temperature is directly related to the exciton binding energy.

The wide gap II-VI and III-V semiconductors combine a large Rabi-splitting energy and a high exciton binding energy of about 20 meV in bulk ZnSe [14] and about 25 meV in bulk GaN (both hexagonal and cubic) [15]. Therefore these materials are particularly suited for microcavity applications such as polariton amplification devices operated at room temperature.

In this paper we review recent experimental investigations of a ZnSe based microcavity containing four strained (Zn,Cd)Se quantum wells and dielectric ZnS and YF_3 distributed Bragg-mirrors (DBRs) [16]. Measurements of the reflectivity and the photoluminescence reveal clear evidence of the strong coupling between the photonic mode (PM) of the resonator and the excitonic mode (EM), yielding a Rabi-splitting energy $\hbar\Omega_{Rabi}$ of about 44 meV at room temperature. We shall also discuss the structural and optical properties of cubic (Al,Ga)N/GaN quantum structures, which may be used in the future for the observation of polariton effect at room temperature.

2 Experimental details

A ZnSe/(Zn,Cd)Se multi quantum well (MQW) structure was grown on (001)-GaAs by molecular beam epitaxy (MBE) (at T = 310 °C). A cavity layer thickness gradient across the sample of about 2 nm per mm sample length was realized by mounting the substrate in an appropriate angle with respect to the effusion cells. Four (Zn,Cd)Se quantum wells with a cadmium content of $x = 0.34 \pm 0.02$ and a thickness of d = 7 nm were placed near the antinodes of the standing wave in the resonator. After the epitaxial growth process, an 8-fold stack of ZnS/YF_3 DBRs was deposited by thermal evaporation on top of the MQW structure. Then the GaAs substrate was removed by wet etching and the microcavity was completed by a 6-fold stack of DBRs on the backside.

The sample was characterized by high resolution X-ray diffraction (HRXRD) in triple axis mode. The structural data were obtained from a simulation of the X-ray spectra using dynamical X-ray diffraction theory [17].

For reflectivity measurements we used a tungsten lamp and a spot of about 100 µm diameter focused on the sample. The photoluminescence (PL) was measured using a HeCd laser at $\lambda = 325$ nm with an excitation density of approximately 1 Wcm^{-2}. Both, reflectivity- and PL spectra were measured on different positions on the sample in order to obtain data as a function of the cavity length.

Cubic $Al_xGa_{1-x}N$/GaN quantum–wells were grown on (001) 3C-SiC substrates by rf-plasma assisted MBE at growth temperatures of 720 °C under stoichiometric growth conditions. The GaN multi-quantum-wells (MQW's) were sandwiched between two 50 nm thick fully strained $Al_xGa_{1-x}N$ layers.

The photoluminescence (PL) was excited by an Ar^+-UV laser at 351 nm. Depht resolved cathodoluminescence (CL) measurements were done under focused conditions using acceleration voltages between 3 and 15 kV and a focussed electron beam.

3 Results and discussion

a) ZnSe/(Zn,Cd)Se microcavities: After the epitaxial growth process, the MQW structure was characterised by HRXRD in order to obtain the important structural parameters such as strain, cavity length LC as well as thickness dQW and mole fraction xCd of the (Zn,Cd)Se QWs. Measurements of reciprocal space maps around the (004)- and (–2–24)-Bragg-reflexes gave detailed information about the strain status. Results are not shown here but yield a partial relaxation of the ZnSe layer on GaAs, while the (Zn,Cd)Se QWs were coherently strained on ZnSe. From the results of the symmetrical map a tilt of the epitaxial layer on the GaAs substrate was excluded. The partial relaxation of the ZnSe layers was estimated to about 40%.

Structural parameters (i.e. thickness and mole fraction of the QWs as well as the cavity length) were obtained from the measurement of an ω–2ϑ-scan as illustrated in Fig. 1 (dots). The spectrum was normalized to the GaAs substrate Bragg-reflex and $\Delta 2\vartheta$ denotes the relative angular difference to the GaAs Bragg-reflex.

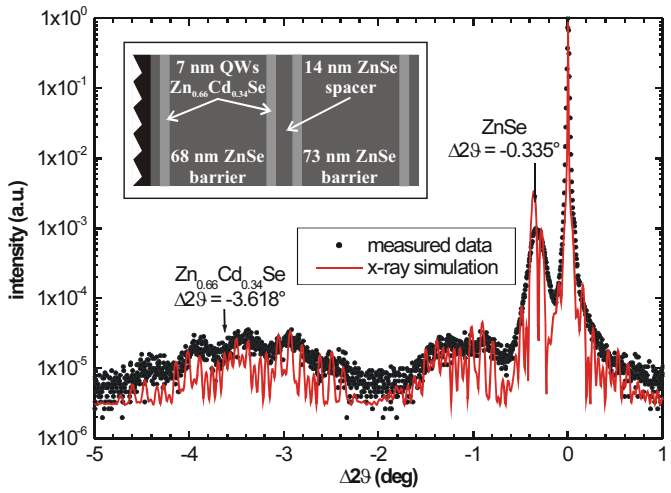

Fig. 1 Dots are experimental data of a X-ray diffraction ω–2ϑ-scan of the MQW sample measured relative to the (004)-GaAs-reflex. The full curve is the result of a dynamic simulation of the experimental data using diffraction theory. The parameters of the sample shown in the inset were obtained from the X-ray simulation.

The full curve represents the dynamic X-ray simulation of the measured spectrum The structural parameters of the MQW structure shown in the small inset of Fig. 1 were used as fitting parameters. We obtained a QW thickness of about $d_{QW} = 7 \pm 0.5$ nm and a cadmium mole fraction of $x_{Cd} = 0.34 \pm 0.02$. The length of the whole MQW structure was calculated to be about $L_C \sim 195$ nm. With the finite barrier model and the structural parameters obtained from Fig. 1 we calculated a QW transition energy of 2.34 eV in good agreement with the experimental results shown in Fig. 2.

A fine tuning of the photonic resonator mode energy (PM) was obtained by varying the spot position on the sample in direction of the cavity length gradient. Fig. 2 depicts room temperature reflectivity spectra of the microcavity near the resonance position (curves A to C), L_C denotes the calculated cavity length. Spectrum D is the microcavity luminescence measured off resonance. Spectra A and B show the photonic mode only, yielding a cavity linewidth of about $\Delta E_P = 16$ meV and a blue-shift with decreasing cavity length. PM and EM approach the resonance condition in spectrum C and a splitting into two absorption peaks with an energy difference of $\hbar\Omega = 41$ meV is resolved. The full curves in Fig. 2 depict the polariton absorption peaks calculated using the Transfer-Matrix model [18, 19]. For this calculation the structural parameters of the MQW structure as well as the EM luminescence at $E_X = 2.313$ eV were used. From the off-resonant microcavity PL mesurements (grey curve in Fig. 2) we obtained EM emission at about $E_X = 2.31$ eV with a linewidth of about $\Delta E_X = 27$ meV. We conclude that the absorption peaks at 2.290 eV and 2.331 eV in spectrum C are due to polariton absorption, yielding a Rabi-splitting energy of about $\hbar\Omega_{Rabi} = 41$ meV.

For further investigation of the photon–exciton coupling in this structure we performed also temperature-dependent PL measurements between 270 K and 330 K. In these experiments the cavity mode energy (PM) was kept constant, while the variation of the temperature leads to a shift of the quantum well emission energy (EM).

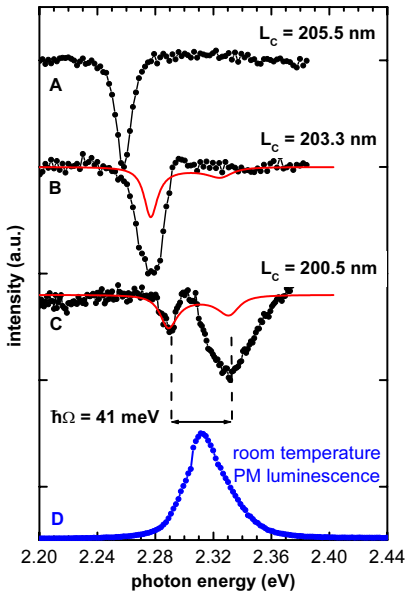

Fig. 2 Room temperature reflectivity spectra of the microcavity structure near the resonance between PM and EM. Spectrum A and B show the cavity mode only, while in C a separation in two absorption peaks with a minimum splitting energy $\hbar\Omega$ = 41 meV is observed. The full curves depict the microcavity reflectivity calculated with the Transfer-Matrix model. Spectrum D is the microcavity luminescence at about E_X = 2.31 eV with a linewidth of about ΔE_X = 27 meV measured off resonance.

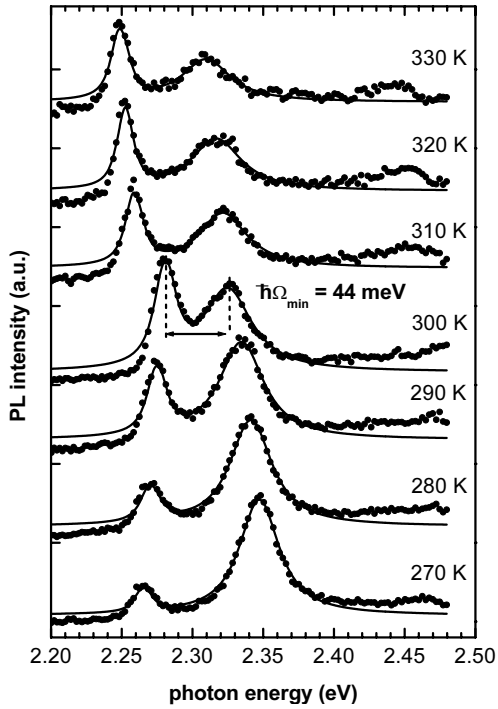

Fig. 3 PL spectra of the microcavity in resonance condition measured between 270 K and 330 K (dots). The full curves represent Lorentzian fits. PM is fixed at E_p = 2,29 keV. The experimental data show a clear "anti-crossing" behavior of the polariton luminescence peaks. A minimum Rabi-splitting of $\hbar\Omega_{min}$ = 44 meV was detected at 300 K.

The PL spectra measured at different temperatures are shown in Fig. 3. With the temperature increasing from 270 K to 330 K the QW emission energy shifts to lower energies with about 1 meVK^{-1}. Therefore the EM approaches a fixed PM (given by the cavity length L_C = 200.5 nm) and reaches the resonance condition at about 300 K. The luminescence peaks show a clear "anti-crossing" behavior. The minimal energy difference between both peaks of about $\hbar\Omega_{min}$ = 44 meV is the Rabi-splitting energy. This value is in good agreement with the experimental results obtained from the reflectivity measurements in Fig. 2 and confirms the existence of the strong coupling at room temperature in our microcavity structure.

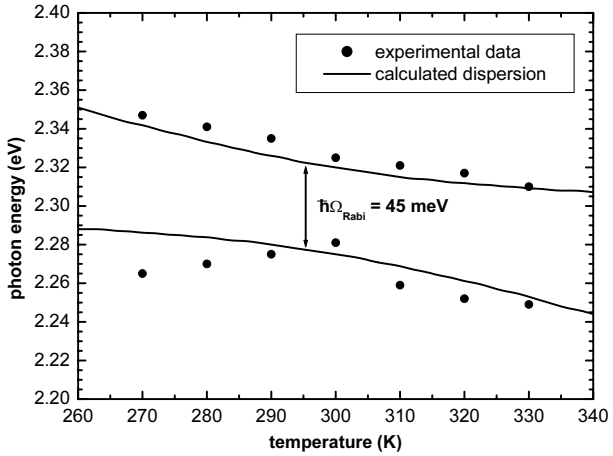

Fig. 4 Polariton luminescence peak energies as a function of temperature (dots). Curves are calculated polariton dispersion branches E_{pol+} and E_{pol-} with a Rabi-splitting energy of $\hbar\Omega_{Rabi}$ = 45 meV.

The dots in Fig. 4 show the peak energies of the polariton luminescence versus temperature. The full curves in Fig. 4 are calculated using a model of the polariton dispersion by André et al. [11]. The polariton dispersion $E_{pol\pm}$ is given by

$$E_{pol\pm} = ½ (E_X + E_P) \pm ½ [\hbar\Omega_{Rabi}^2 + (E_X - E_P)^2]^2 \quad (1)$$

where E_X and E_P are the uncoupled dispersions of the EM and the PM, respectively and $\hbar\Omega_{Rabi}$ is the Rabi-splitting energy. The parameters which were used in the calculation are E_X = 2.627–1.1 x 10^{-3} eV for the temperature dependence of the QW emission and E_P = 2.298 eV for the cavity mode energy, respectively. The fitting procedure yields $\hbar\Omega_{Rabi}$ = 45 meV, which is in good agreement with our experimental results.

The "splitting-to-linewidth-ratio" is an important condition to achieve strong coupling. The Rabi-splitting energy must exceed the averaged linewidth of PM and EM

$$½ (\Delta E_X + \Delta E_P) < \hbar\Omega_{Rabi}. \quad (2)$$

In case of our microcavity we calculated an averaged linewidth of about 22 meV. This results in a "splitting-to-linewidth-ratio" of about $\hbar\Omega_{Rabi} / (\Delta E_X + \Delta E_P) \approx 2$ and the condition (2) is sufficiently fulfilled.

b) Cubic GaN and AlN based microcavities: In cubic GaN-based III–V microcavities the Rabi-splitting energy is expected to be significantly larger than in ZnSe [20]. This fact reduces the demands regarding the FWHM value of photonic and excitonic mode. As preliminary work on c-GaN-based microcavity structures we investigated cubic (Al,Ga)N/GaN MQW structures grown on SiC substrate. The cross-section of a typical sample structure is depicted in Fig. 5. Five GaN QWs with a thickness of about 3 nm are enclosed in 6 nm (Al,Ga)N barriers with a nominal aluminium mole fraction of about x_{Al} = 0.15. The active layer is sandwiched between

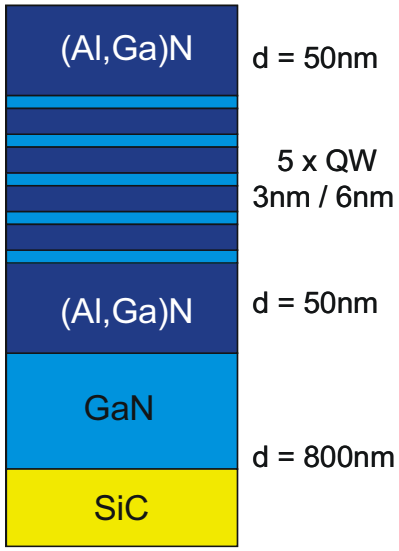

Fig. 5 (Al,Ga)N/GaN MQW structure grown on a GaN buffer layer of about 800 nm thickness. The 3 nm thick GaN QWs are enclosed between 6 nm (Al,Ga)N barriers with a nominal aluminium mole fraction of about 0.15.

two (Al,Ga)N barriers with a nominal layer thickness of 50 nm. The whole quantum structure is grown on a GaN buffer with a thickness of about 800 nm.

Figure 6 depicts the reciprocal space map of the (–1–13)-Bragg reflex of the MQW structure. The Bragg-reflex of the GaN buffer as well as the (Al,Ga)N barriers are clearly resolved in the spectrum. The calculated reciprocal lattice parameters of GaN, AlN and AlN strained on GaN are also illustrated in the map. The map shows that the (Al,Ga)N barriers are pseudomorph to the GaN buffer. The AlN mole fraction is 0.15.

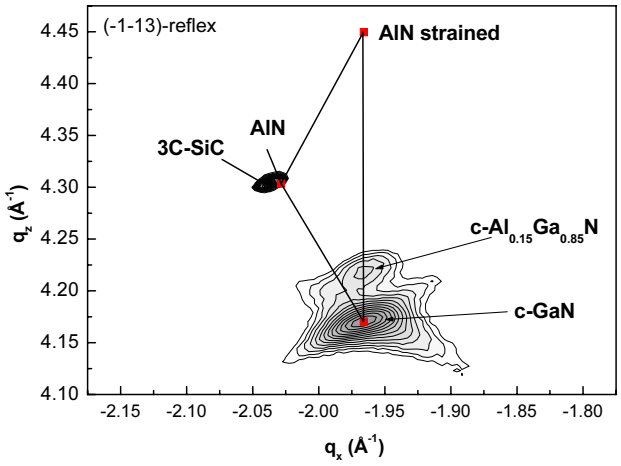

Fig. 6 Reciprocal space map of the (–1–13)-reflex of the (Al,Ga)N/GaN MQW structure. The (Al,Ga)N barriers are fully strained on the GaN buffer layer.

The FWHM value of the (Al,Ga)N rocking curve (about 29 arcmin) is close to that of the GaN buffer layer (about 26 arcmin). Notably, the typical rocking curve FWHM value of partial relaxed (Al,Ga)N is about two times larger compared to these result.

Figure 7 shows the photoluminescence spectrum of the MQW excited with an Ar^+-Laser. The QW emission was clearly resolved at about E = 3.31 eV and a linewidth of ΔE = 102 meV was observed. The weak luminescence detected at about 3.21 eV is related to the bandgap emission of the GaN buffer layer. With the finite barrier model we calculated the QW transition energy to about E_{QW} = 3.291 eV using the structural parameters given in Fig. 5 and Fig. 6. This value is in good agreement with the experimental results.

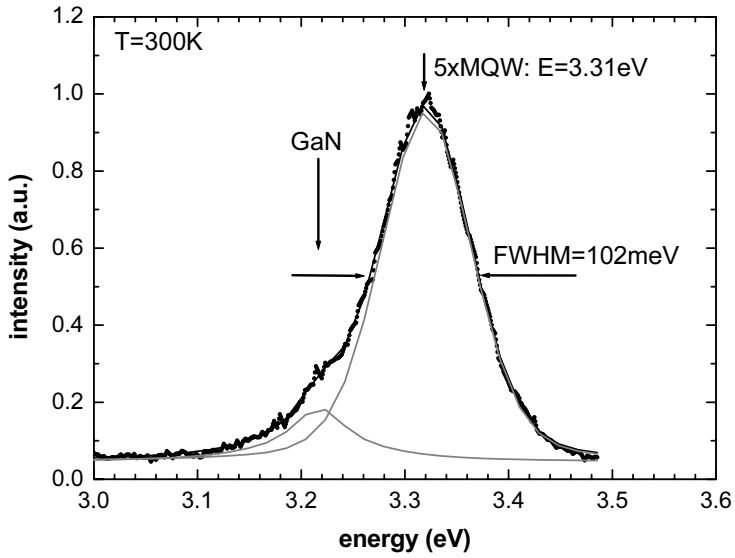

Fig. 7 Room temperature photoluminescence spectrum of a cubic-AlGaN/GaN MQW structure. The QW transition energy is E = 3.31 eV and the linewidth is about 102 meV. The GaN buffer layer luminescence at 3.21eV is relatively weak.

The linewidth of the (Al,Ga)N/GaN QW emission is one of the smallest measured with cubic III-nitrides. Considering the Rabi-splitting energy of bulk h-GaN, which has recently been measured [19] and a comparable cavity mode linewidth as a guide number, the "splitting-to-linwidth-ratio" condition for the strong coupling at room temperature will be sufficiently fulfilled with an 9-fold (Al,Ga)N/GaN MQW structure.

4 Conclusions

In conclusion, we have observed strong exciton–photon coupling in ZnSe/(Zn,Cd)Se MQW microcavities, which were covered by dielectric Bragg-mirrors yielding a room temperature Rabi splitting of 44 meV. To our knowledge this is the largest Rabi splitting measured at room temperature with an inorganic semiconductor microcavity. We also report first results of experiments with cubic AlGaN/GaN quantum wells revealing that cubic III-nitride microcavity structures are promising for the realization of future low threshold photonic devices which exploit the bosonic nature of polaritons and work at room temperature.

References

[1] J.M. Gérard, B. Sermage, B. Legrand, E. Costard, and V. Thierry-Mieg, Phys. Rev. Lett. **81**, 1110 (1998).
[2] J.J. Baumberg, Physics World, March 2002, p. 37.
[3] G. Malpuech, A.D. Carlo, A. Kavokin, J.J. Baumberg, M. Zamfirescu, and P. Lugli, Appl. Phys. Lett. **81**, 412 (2002).
[4] C. Weisbuch, M. Nishioka, A. Ishikawa, and Y. Arakawa, Phys. Rev. Lett. **69**, 2132 (1992).
[5] C. Weisbuch, H. Benisty, and R. Houdré, J. Lumin. **85**, 271 (2000).
[6] M.V. Artemyev and U. Woggon, Appl. Phys. Lett. **76**, 1353 (2000).
[7] G. Khitrova and H.M. Gibbs, F. Jahnke, M. Kira, and S.W. Koch, Rev. Mod. Phys. **71,** 1591 (1999).
[8] L.S. Dang, D. Heger, R. André, F. Bœuf, and R. Romestain, Phys. Rev. Lett **81**, 3920 (1998).
[9] J.H. Dickerson and E.E. Mendez, A.A. Allerman, S. Manotas, F. Agulló-Rueda, and C. Pecharromán, Phys. Rev. B **64**, 155302 (2001).
[10] P. Kelkar, V. Kozlov, H. Jeon and A.V. Nurmikko, C.-C. Chu, D.C. Grillo, J. Han, C.G. Hua, and R.L. Gunshor, Phys. Rev. B **52**, R5491 (1995).
[11] R. André, F. Bœuf, R. Romestain, Le Si Dang, E. Péronne, J.F. Lampin, D. Hulin, and A. Alexandrou, J. Cryst. Growth **214/215**, 1002 (2000).
[12] M. Saba, C. Ciuti, S. Kundermann, J.L. Staehli, B. Deveaud, J. Bloch, V. Thierry-Mieg, R. André, Le Si Dang, G. Bongiovanni, and A. Mura, phys. stat. sol. (a) **190**, 315 (2002).
[13] M. Saba, C. Ciuti, J. Bloch, V. Thierry-Mieg, R. André, Le Si Dang, S. Kundermann, A. Mura, G. Bongiovanni, J.L. Staehli, and B. Deveaud, Nature **414**, 731 (2002).
[14] H.E. Gumlich, D. Theis, and D. Tschierse (O. Madelung, Landolt Börnstein, eds.), New Series, Group III, Vol. 17b (Springer-Verlag, Berlin, 1982) .
[15] D.J. As, F. Schmilgus, C. Wang, B. Schöttker, D. Schikora, and K. Lischka, Appl. Phys. Lett. **70**, 1311 (1997)
[16] A. Pawlis, A. Khartchenko, O. Husberg, D.J. As, K. Lischka, and D. Schikora, Sol. State Comm. **123**, 235 (2002)
[17] A. Pawlis, A. Khartchenko, O. Husberg, D. Schikora, and K. Lischka, phys. stat. sol. (a) **188**, 983 (2001).
[18] A. Tredicucci, Y. Chen, V. Pellegrini, M. Börger, and F. Bassani, Phys. Rev. A **54**, 3493 (1996).
[19] S.H. Wemple and M. DiDomenico, Jr., Phys. Rev. B **3**, 1339 (1971).
[20] N. Antoine-Vincent, F. Natali, D. Byrne, A. Vasson, P. Disseix, J. Laymarie, M. Leroux, F. Semond, and J. Massies, Phys. Rev. B **68**, 153313 (2003).